Double, triple and multiple impulses for critical elastic-plastic earthquake response analysis to near-fault and long-duration ground motions

I. Takewaki
Kyoto University, Kyoto, Japan

K. Kojima
Kyoto University, Kyoto, Japan

ABSTRACT: Near-fault ground motions and long-period, long-duration ground motions possess special characteristics. The essential aspect of the near-fault ground motions can be characterized by one-cycle or a few-cycle sinusoidal waves (e.g. Ricker wavelet) which are well represented by double or triple impulses. Furthermore, the principal part of the long-period, long-duration ground motions can be characterized by many-cycle sinusoidal waves which are well described by multiple impulses. In this paper, it is shown that good approximate elastic-plastic responses of various structural models to the near-fault ground motions and long-period, long-duration ground motions can be derived by using the responses to the double, triple and multiple impulses. The energy approach plays an important and critical role in the derivation of such good approximate responses in closed form.

1 INTRODUCTION

It is well known that near-fault ground motions have peculiar characteristics and long-period, long-duration ground motions are causing great influences on high-rise buildings and base-isolated buildings. The effects of near-fault ground motions on structural response have been investigated extensively (Hall et al. 1995, Sasani and Bertero 2000, Alavi and Krawinkler 2004, Kalkan and Kunnath 2006, Khaloo et al. 2015). The fling-step and forward-directivity are two special keywords to characterize such near-fault ground motions (Mavroeidis and Papageorgiou 2003, Kalkan and Kunnath 2006). Especially, Northridge earthquake in 1994, Hyogoken-Nanbu (Kobe) earthquake in 1995 and Chi-Chi (Taiwan) earthquake in 1999 raised special attention to many earthquake structural engineers.

The fling-step and forward-directivity inputs have been characterized by two or three wavelets. For this class of ground motions, many useful research works have been conducted. Mavroeidis and Papageorgiou (2003) investigated the characteristics of this class of ground motions in detail and proposed some simple models. In this paper, several new approaches based on the double impulse (Kojima and Takewaki 2015a) and the triple impulse (Kojima and Takewaki 2015b) are proposed for various models representing important nonlinear vibration phenomena and the intrinsic response characteristics by the near-fault ground motion are captured. Then the approaches are applied to several interesting models in practice (soil-structure interaction problem, dynamic stability problem including collapse, overturning problem of rocking block). The common concept is the modeling of simple sinusoidal waves into a few impulses and the use of energy balance in the closed-form derivation of the maximum elastic-plastic response. The use of energy balance is enabled because the impulses cause only free vibration and complicated treatment by forced input can be avoided. The proposed approach is expected to overcome the difficulty of computational repetition for capturing resonant phenomena in nonlinear structural dynamics (Caughey 1960, Iwan 1961).

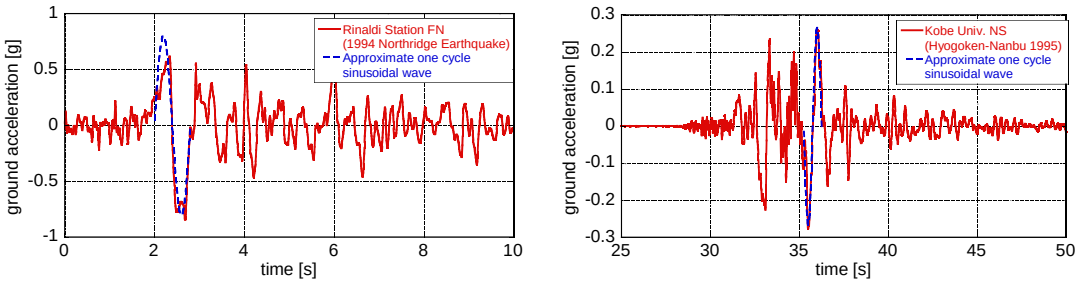

(a) (b)

Figure 1. Modeling of main part of pulse-type recorded ground motion into the corresponding one-cycle sinusoidal input: (a) Rinaldi station fault-normal component (Northridge earthquake 1994), (b) Kobe University NS component (almost fault-normal) (Hyogoken-Nanbu (Kobe) earthquake 1995) (Kojima and Takewaki 2016a)

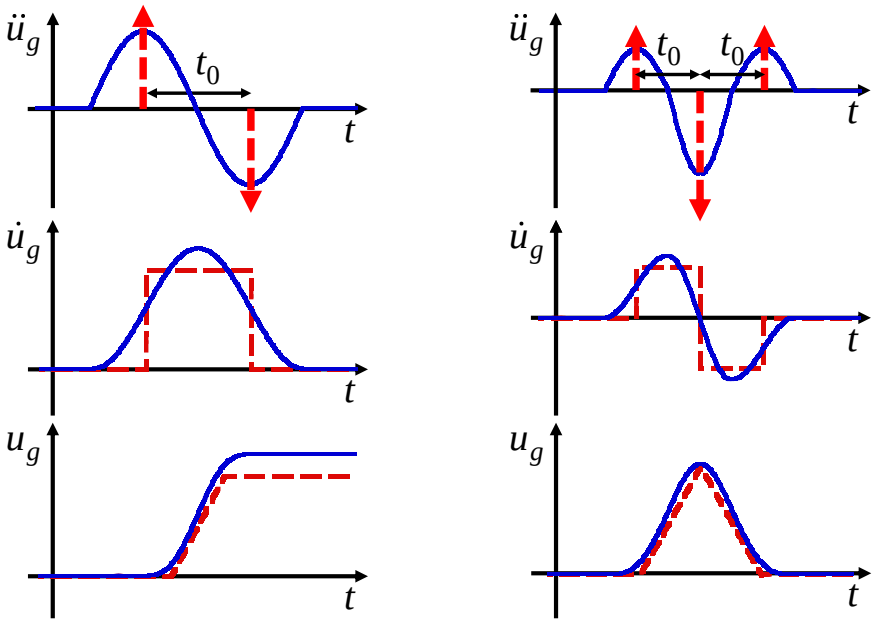

(a) (b)

Figure 2. Modeling of pulse-like ground motions: (a) Fling-step input (one-cycle sine) and double impulse, (b) Forward-directivity input (one and half-cycle sine) and triple impulse (Kojima and Takewaki 2015a)

2 MODELING OF MAIN PART OF NEAR-FAULT GROUND MOTION INTO DOUBLE IMPULSE AND TRIPLE IMPULSE

It is known that most near-fault ground motions have a few pulse-like waves as shown in Figure 1. When only the maximum response is concerned, the response resulting from such pulse-like waves is important. In this paper, the main part of the pulse-like ground motions is modeled into the double impulse (see Figure 2(a)) or the triple impulse (see Figure 2(b)).

In this paper, the level of the double or triple impulse is adjusted so that the maximum Fourier amplitude of the double or triple impulse is equal to that of the corresponding one-cycle sine wave or one and half-cycle sine wave. This adjustment is made in order to guarantee the better response correspondence between the one-cycle sine wave or one and half-cycle sine wave and the double or triple impulse. The correspondence of the Fourier amplitudes between the one-cycle sine wave or one and half-cycle sine wave and the double or triple impulse is shown in Figures 3(a), (b).

3 CLOSED-FORM ELASTIC-PLASTIC RESPONSE TO CRITICAL DOUBLE IMPULSE

Figure 4 shows an overview of the response process of an elastic-perfectly plastic single-degree-of-freedom (SDOF) model to the critical double impulse. The critical double impulse means the double impulse causing the maximum response under a constant velocity amplitude and a variable impulse interval (Drenicl 1970, Takewaki 2007). It should be emphasized that the critical timing of the second impulse is the time when the restoring force attains zero in the first unloading process (Kojima and Takewaki 2015a). The response correspondence (restoring force-deformation relation) under the double impulse is shown in Figure 3(c).

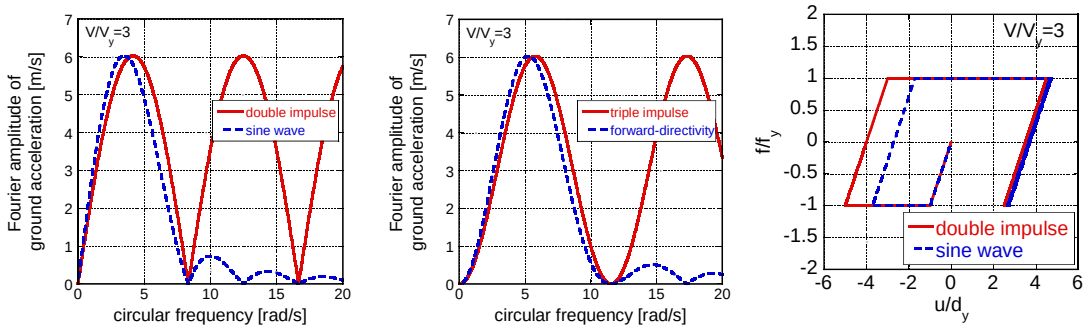

Figure 3. Adjustment of input level of double or triple impulse to the corresponding one-cycle or one and half-cycle sine wave based on Fourier amplitude equivalence and response correspondence under double impulse: (a) Double impulse, (b) Triple impulse, (c) Restoring force-deformation correspondence under double impulse (Kojima and Takewaki 2015a, b)

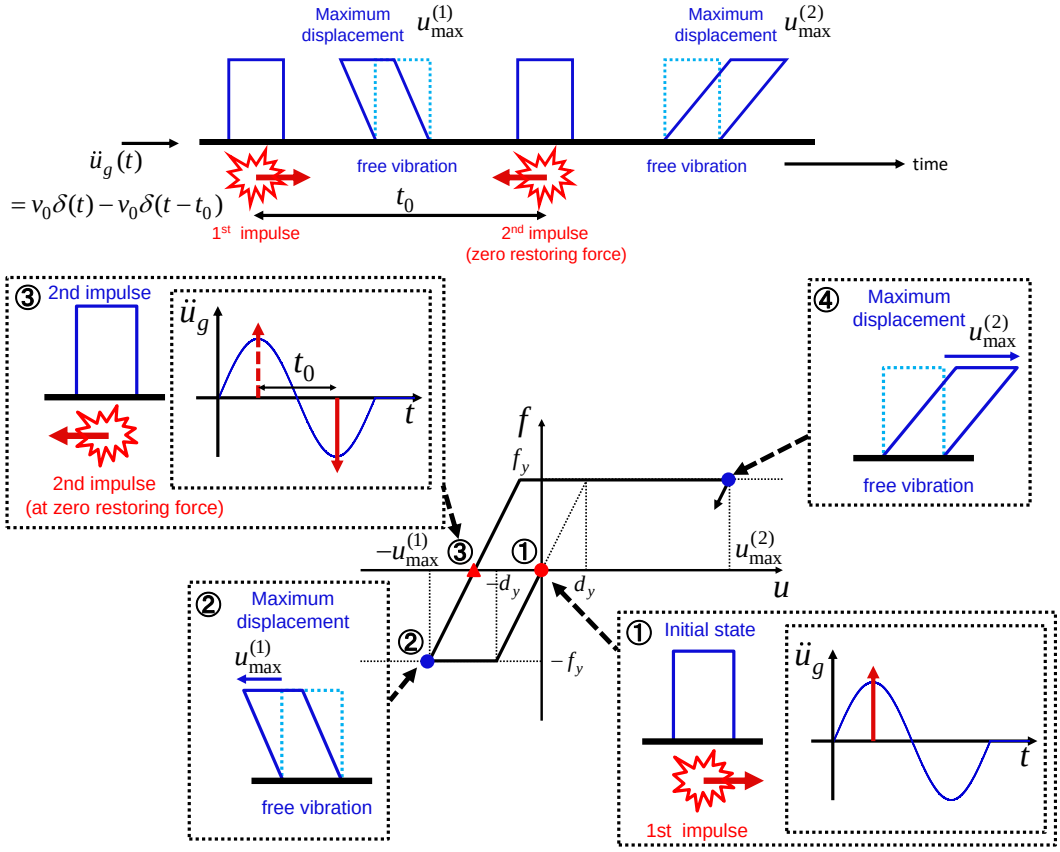

Figure 4. Overview of elastic-plastic response process of SDOF model to critical double impulse (Critical timing of second impulse is the time when the restoring force attains zero in the first unloading process.)

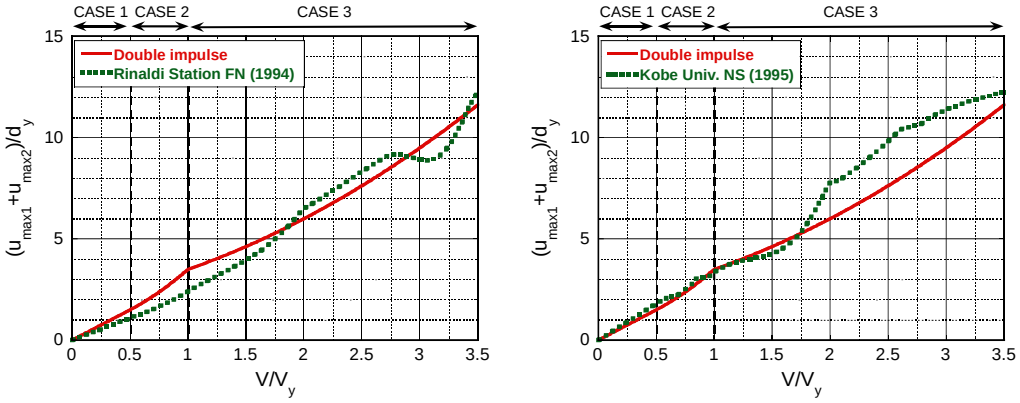

Figure 5. Maximum amplitude of deformation for the recorded ground motions and the proposed one: (a) Rinaldi station fault-normal component, (b) Kobe University NS component (Kojima and Takewaki 2016a)

Figure 5 illustrates the maximum deformation for two recorded ground motions (Rinaldi station fault-normal component during Northridge earthquake 1994 and Kobe University NS component during Hyogoken-Nanbu (Kobe) earthquake 1995) and that obtained by the proposed critical double impulse. Since the recorded ground motion is fixed, the initial velocity V is fixed and V_y (product of the natural circular frequency ω_1 and the yield deformation d_y: reference velocity giving just yield deformation after the first impulse) is changed here. Because ω_1 is closely related to the resonance condition, d_y is changed principally. This procedure is similar to the well-known elastic-plastic response spectrum developed in 1960-1970 in the field of earthquake resistant design. The solid line is obtained by changing V_y for the specified V using the method for the double impulse and the dotted line is drawn by conducting the elastic-plastic time-history response analysis on each model with varied V_y under the recorded ground motion. It can be observed that the result by the proposed method is a fairly good approximation of the recorded pulse-type ground motions. If we use a bilinear hysteresis model with a positive second slope, the correspondence becomes better.

4 CLOSED-FORM ELASTIC-PLASTIC RESPONSE TO CRITICAL TRIPLE IMPULSE

In comparison with the response to the double impulse, the process of deriving the critical timing is somewhat complicated in the triple impulse. The maximum deformation after the first impulse is denoted by $u_{\max 1}$, that after the second impulse is expressed by $u_{\max 2}$ and that after the third impulse is described by $u_{\max 3}$. The maximum deformation can be obtained by using the energy balance of kinetic energy, strain energy and dissipated energy.

Figure 6 shows the following four cases depending on the input level.

CASE 1: Elastic response during all response stages ($u_{\max 3}$ is the largest)

CASE 2: Yielding after the third impulse ($u_{\max 3}$ is the largest)

CASE 3: Yielding after the second impulse ($u_{\max 2}$ or $u_{\max 3}$ is the largest)

3-1: The timing of the third impulse is in the unloading stage.

3-2: The timing of the third impulse is in the yielding (loading) stage.

CASE 4: Yielding after the first impulse ($u_{\max 2}$ is the largest)

It is assumed here that the critical impulse has the second impulse timing (time of the second impulses) of zero restoring force in the first unloading process. It can be understood that the third impulse timings (time of the third impulses) are different in CASE 3 and CASE 4. Careful treatment should be made in the derivation of the critical timing (Kojima and Takewaki 2015b).

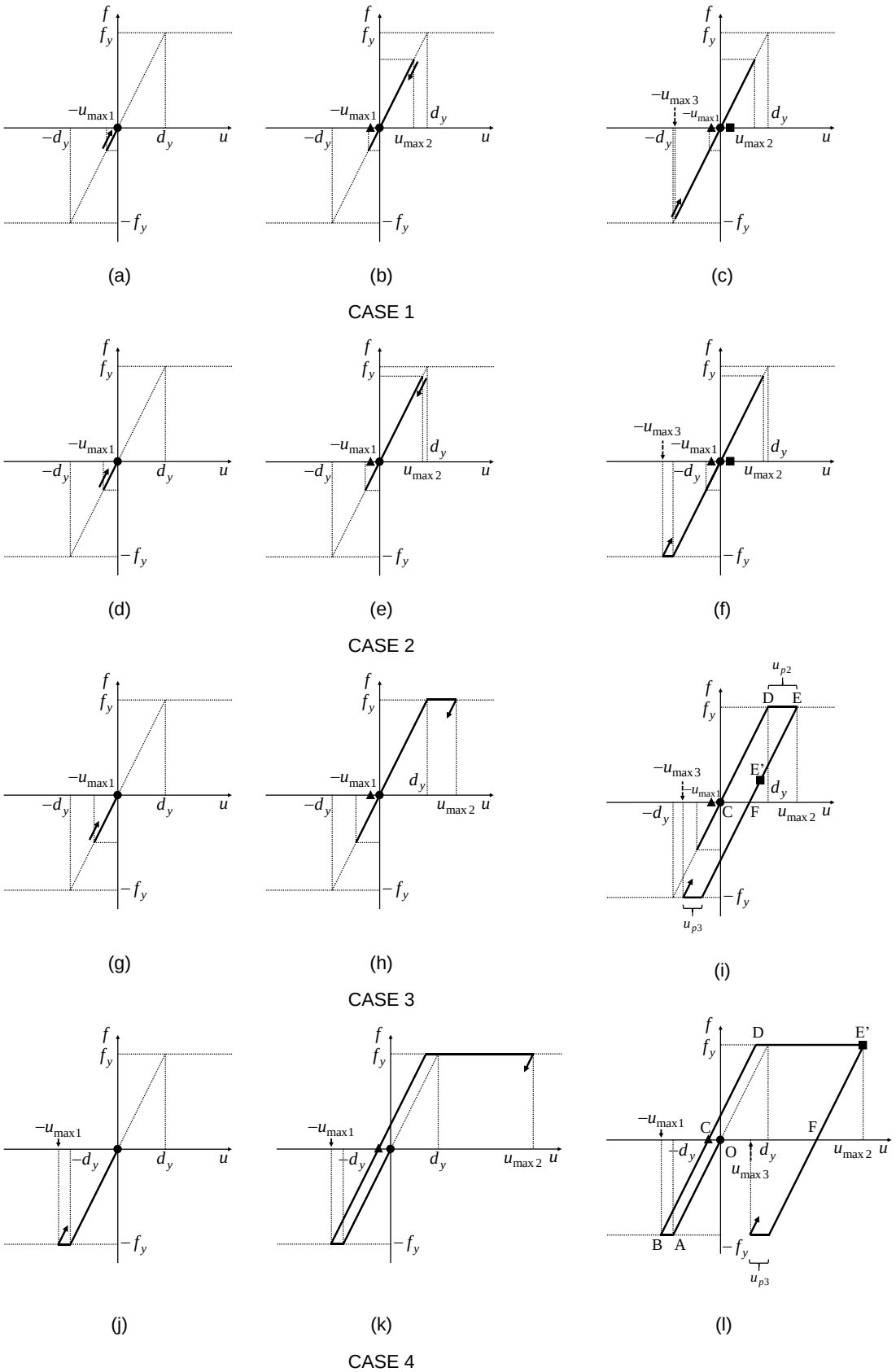

Figure 6. Prediction of maximum elastic-plastic deformation under triple impulse based on energy approach (● : first impulse, ▲ : second impulse, ■: third impulse) (Kojima and Takewaki 2015b)

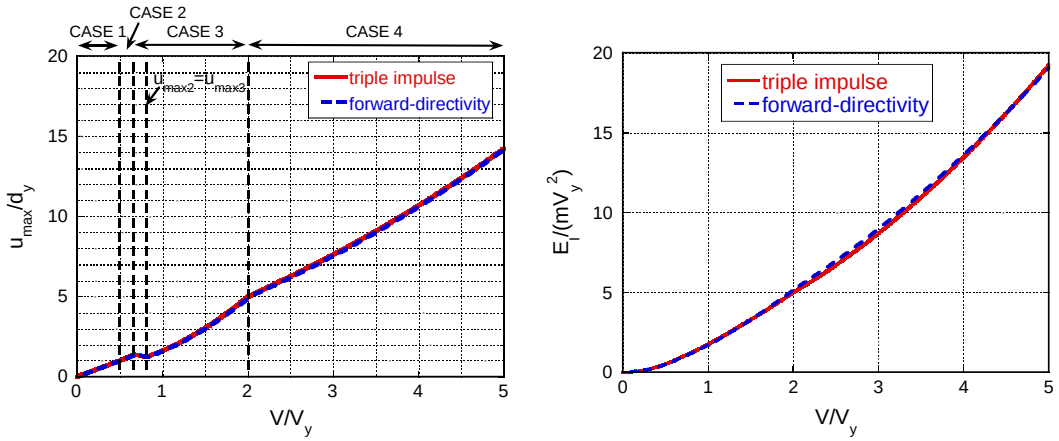

Figure 7. Comparison of triple impulse and the corresponding three wavelets of sinusoidal waves: (a) Ductility, (b) Earthquake input energy (Kojima and Takewaki 2015b)

Figure 7 shows the comparison of critical ductility and earthquake input energy between the triple impulse and the forward-directivity input (one and half-cycle sine wave). It can be observed that, when the adjustment of input amplitude is made following the procedure in Section 2, the responses of the triple impulse and the forward-directivity input coincide fairly well.

5 CLOSED-FORM CRITICAL EARTHQUAKE RESPONSE OF ELASTIC-PLASTIC STRUCTURES ON COMPLIANT GROUND UNDER NEAR-FAULT GROUND MOTIONS

The problem of soil-structure interaction is very interesting and important in the structural and geotechnical engineering. It is aimed here that, once the soil-structure interaction model can be modeled into an SDOF model, the formulation presented in Section 3 can be applied to the soil-structure interaction model. Figure 8 presents the simplified swaying-rocking model and the equivalent SDOF model. k_e is the equivalent stiffness.

Figure 9 shows the relation of the maximum deformation ratio $(d_y+u_p)/d_y$ (d_y: yield deformation, u_p: plastic deformation) with V/V_y for three soil conditions and fixed-base case. In the low input level, as the ground becomes stiffer, the plastic deformation of the super-structure becomes larger. On the other hand, in the large input level, as the ground becomes softer, the plastic deformation of the super-structure becomes larger. These properties result from the fact that, as the ground becomes softer, the strain energy stored in the ground becomes larger in the case where the super-structure is in the plastic range. It is interesting to note that such properties can be derived by taking full advantage of the closed-form expression of the critical elastic-plastic responses (Kojima and Takewaki 2016a).

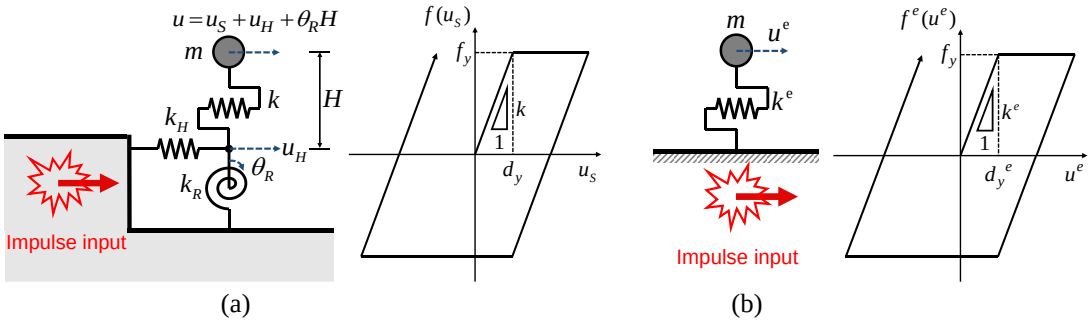

Figure 8. Modeling in soil-structure interaction problem:
(a) Simplified swaying-rocking model, (b) Equivalent SDOF model (Kojima and Takewaki 2016a)

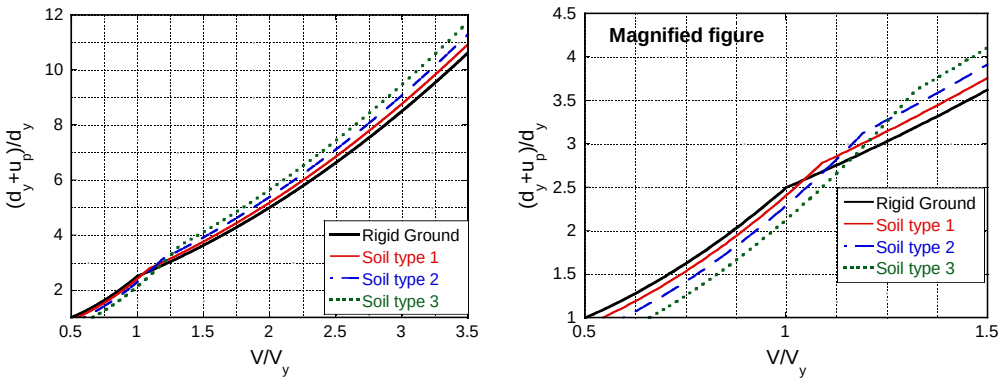

Figure 9. Relation of the maximum plastic deformation $(d_y + u_p)/d_y$ with V/V_y for three soil conditions and fixed-base case (Kojima and Takewaki 2016a)

6 CLOSED-FORM DYNAMIC STABILITY CRITERION FOR ELASTIC-PLASTIC STRUCTURES UNDER NEAR-FAULT GROUND MOTIONS

The problem of dynamic collapse of structures has been an important and challenging problem for long time. In this section, it is demonstrated that the proposed approach (balance of input energy and dissipated energy) can be applied to this problem. Figure 10 shows several patterns of stability limit (patterns of collapse). The vertical axis is the ratio of the input velocity level to the structural strength and the horizontal axis is the second slope ratio to the first stiffness. A more detailed derivation can be found in the reference (Kojima and Takewaki 2016b).

Figure 11(a) shows the maximum deformation with respect to V/V_y under the Rinaldi station fault-normal component and the corresponding double impulse. The solid line has been drawn by the proposed method. On the other hand, the dotted line has been obtained from the time-history response analysis for many models with different values of V_y. It can be found that about $V/V_y = 0.8$ is the approximate limit. From the detailed investigation, $V/V_y = 0.78$ and $V/V_y = 0.79$ have been selected for candidates to be investigated. Figure 11(b) demonstrates the restoring-force-deformation relation for the stable case ($V/V_y = 0.78$) and the unstable case ($V/V_y = 0.79$). In addition, Figure 11(c) presents the deformation time-history for the stable case ($V/V_y = 0.78$) and the unstable case ($V/V_y = 0.79$). On the other hand, Figure 11(d) shows the corresponding restoring-force time-history for stable case ($V/V_y = 0.78$) and the unstable case ($V/V_y = 0.79$). It can be confirmed that the proposed stability limit using the double impulse is fairly accurate.

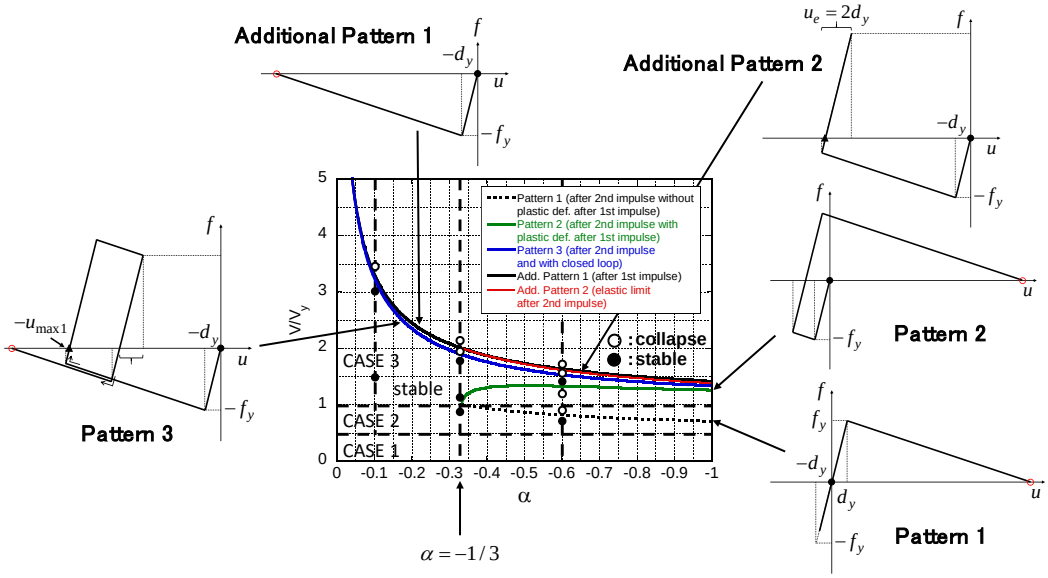

Figure 10. Several patterns of stability limit (patterns of collapse) (Kojima and Takewaki 2016b)

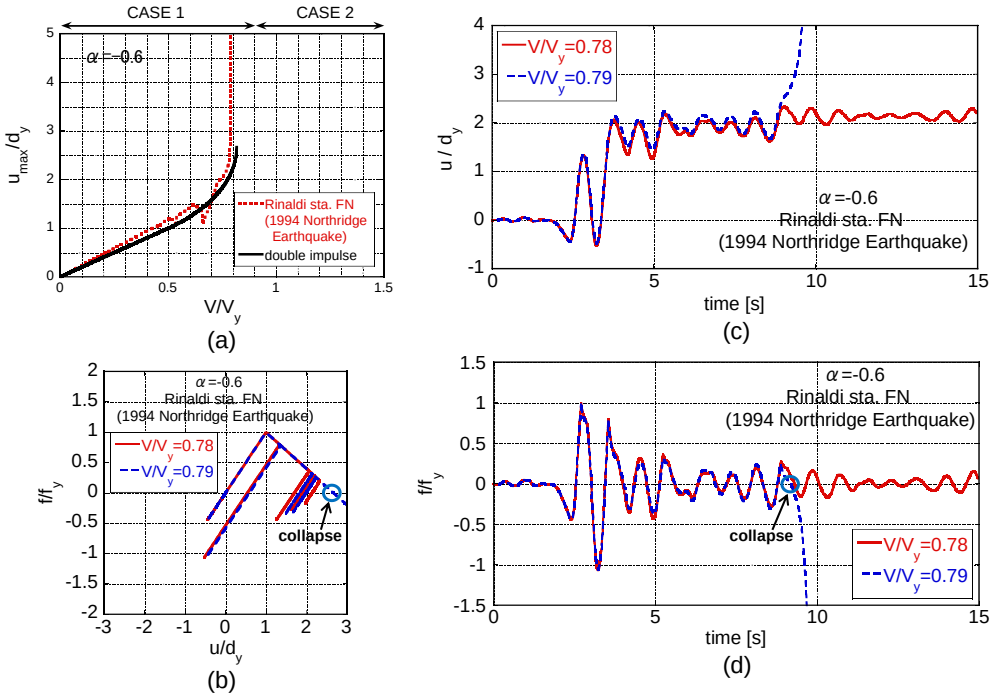

Figure 11. Stable model ($V/V_y = 0.78$) and unstable model ($V/V_y = 0.79$) under Rinaldi station fault-normal component: (a) Maximum deformation with respect to V/V_y under Rinaldi station fault-normal component and the corresponding double impulse, (b) Restoring force-deformation relation for stable case and unstable case, (c) Deformation time-history for stable case and unstable case, (d) Restoring-force time-history for stable case and unstable case (Kojima and Takewaki 2016b)

7 CLOSED-FORM OVERTURNING LIMIT OF RIGID BLOCK UNDER CRITICAL NEAR-FAULT GROUND MOTIONS

A closed-form limit on the input level of the double impulse as a substitute of a near-fault ground motion can be derived for the overturning of a rigid block (Nabeshima et al. 2016). Figure 12 shows the modeling of the rocking motion of a rigid block using a rigid bar supported by a non-linear elastic rotational spring with rigid initial stiffness and negative second slope.

Figure 13 presents the rocking response of a rigid block and governing law (conservation of angular momentum, conservation of energy, energy dissipation).

Figure 14 illustrates the limit velocity amplitude of the critical double impulse with respect to R for $2b$=1, 2, 4[m] (closed-form expression and numerical simulation). The proposed closed-form limit velocity amplitude coincides fairly well with the numerical simulation result. Figure 14 demonstrates that the proposed method seems reliable.

Figure 15 shows the critical acceleration amplitude ratio of the equivalent one-cycle sinusoidal input to acceleration of gravity for $2b$=1, 2, 4[m] and the comparison with other results (Dimitrakopoulos and DeJong 2012, Makris and Kampas 2016). The accuracy of the proposed method can be assured.

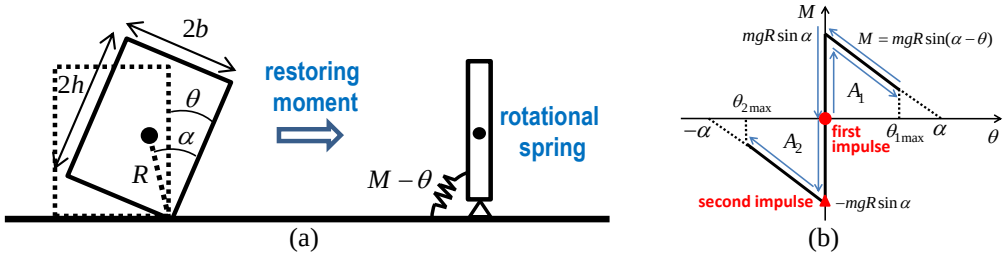

Figure 12. Modeling of rocking rigid block: (a) Modeling by rigid bar supported by non-linear elastic rotational spring with rigid initial stiffness and negative second slope, (b) Moment-rotation relation for rocking response of rigid block and timing of double impulse

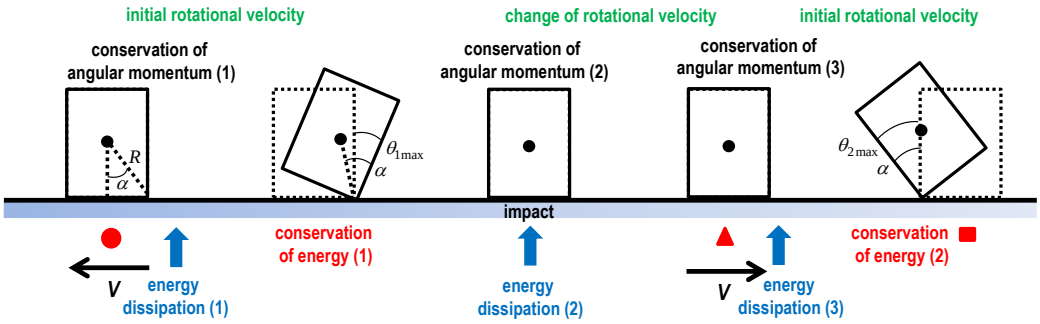

Figure 13. Rocking response of rigid block and governing law (conservation of angular momentum, conservation of energy, energy dissipation) (Nabeshima et al. 2016)

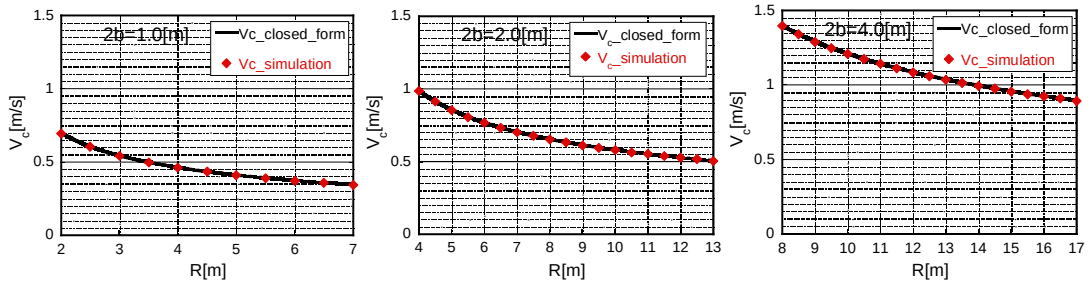

Figure 14. Limit velocity amplitude of critical double impulse with respect to R for $2b$=1, 2, 4[m] (closed-form expression and numerical simulation)

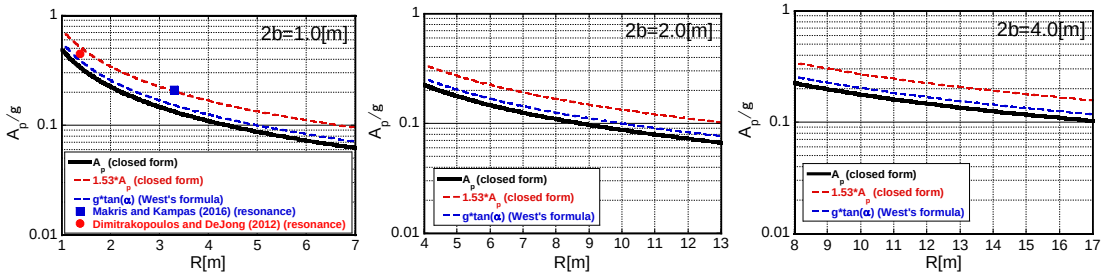

Figure 15. Critical acceleration amplitude ratio of equivalent one-cycle sinusoidal input to acceleration of gravity for $2b$=1, 2, 4[m] and comparison with other results (Nabeshima et al. 2016)

8 SIMPLE EVALUATION METHOD OF SEISMIC RESISTANCE OF RESIDENTIAL HOUSE UNDER TWO CONSECUTIVE SEVERE GROUND MOTIONS

In the 2016 Kumamoto earthquake in Japan, two severe ground shakings with the seismic intensity 7 (the highest level in Japan Metheorological Agency (JMA) scale; approximately X-XII in Mercalli scale) occurred consecutively on April 14 and April 16. In the seismic regulations of most countries, it is usually prescribed that such severe earthquake ground motion occurs once in the working period of buildings. A simple evaluation method has been proposed on the seismic resistance of residential houses under two consecutive severe ground motions with intensity 7 (Kojima and Takewaki 2016c). In that paper, an impulse of the velocity V has been adopted as a representative of near-fault ground motion and two separated impulses have been used as the repetition of intensive ground shakings with the seismic intensity 7 (see Figure 16).

Figure 17 presents the collapse scenario under two impulses and energy consideration for evaluating limit input velocity. Figure 18 illustrates the $V_y^{[2]}/V_y^{[1]}$ for the second-slope ratio α where $V_y^{[1]}$ denotes the reference velocity (strength of the model) just collapsing after one impulse and $V_y^{[2]}$ denotes the reference velocity (strength of the model) just collapsing after two impulses. Finally the plot of $f_y^{[2]}/f_y^{[1]}$ (the ratio of the model strength for just collapse after two impulses to that for just collapse after one impulse) is shown in Figure 19. The simulation using the Kumamoto earthquake ground motion (on April 16) is also included.

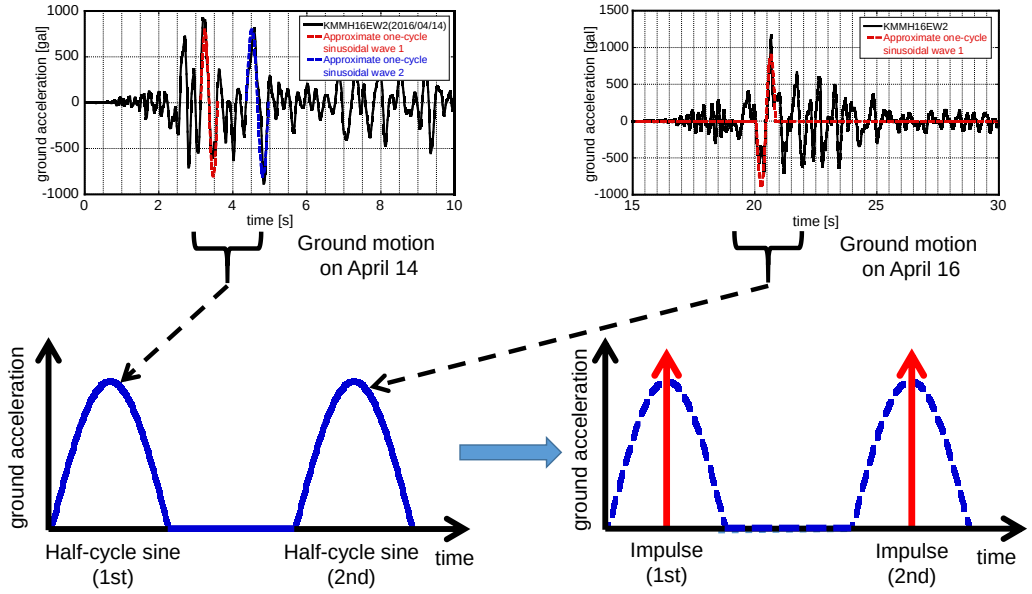

Figure 16. Modeling of repeated intensive ground motions into two impulses
(Kojima and Takewaki 2016c)

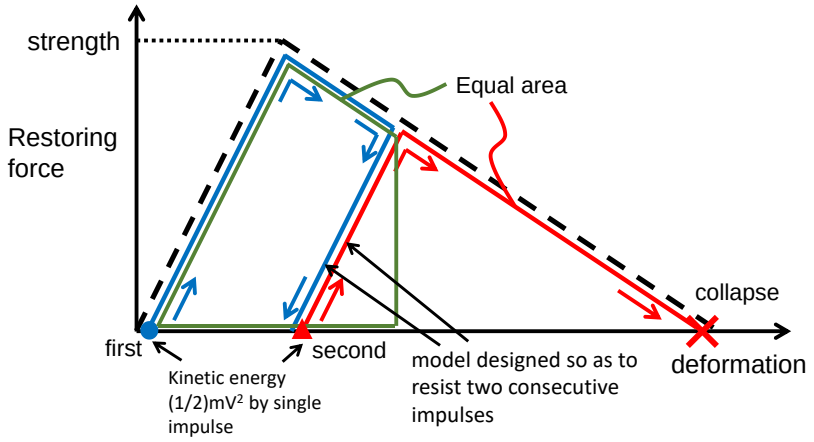

Figure 17. Collapse scenario under two impulses and energy consideration for evaluating limit input level
(Kojima and Takewaki 2016c)

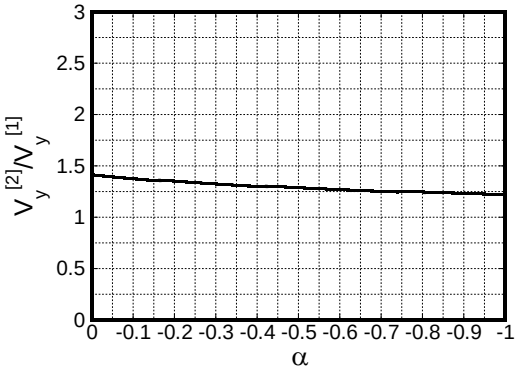

Figure 18. $V_y^{[2]}/V_y^{[1]}$ for α
(Kojima and Takewaki 2016c)

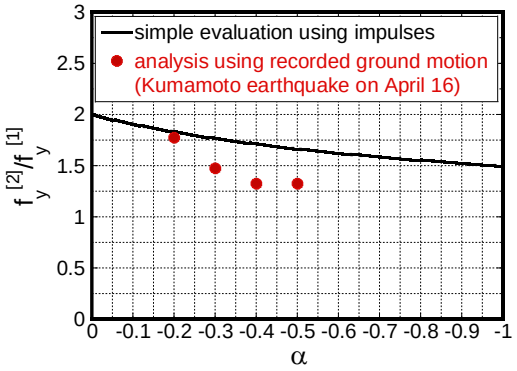

Figure 19. $f_y^{[2]}/f_y^{[1]}$ for α
(Kojima and Takewaki 2016c)

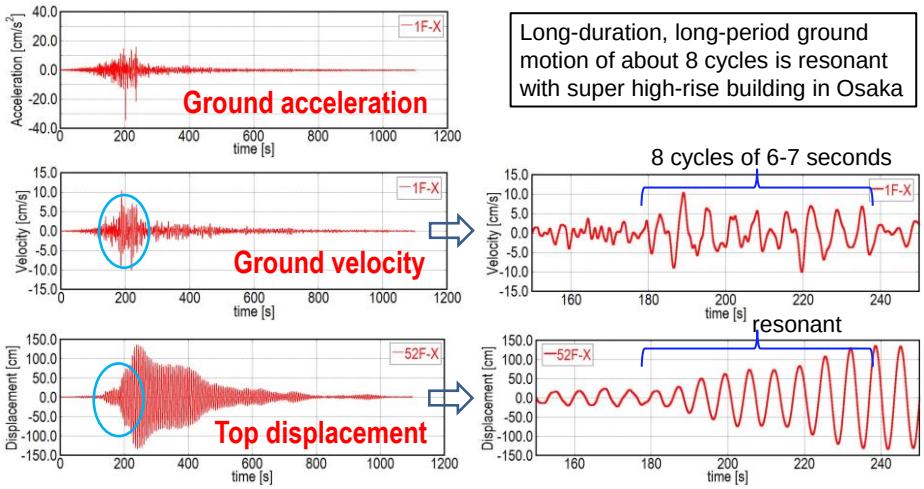

Figure 20. Resonant response of a super high-rise building in Osaka, Japan during the 2011 Tohoku (Japan) earthquake under long-duration, long-period ground motion (Kojima and Takewaki 2015c)

9 CLOSED-FORM ELASTIC-PLASTIC RESPONSE TO CRITICAL MULTIPLE IMPULSE

Long-period, long-duration ground motions are of great concern recently after the Mexico earthquake in 1985, the Tokachioki earthquake in 2003 and the Tohoku (Japan) earthquake in 2011 (Kojima and Takewaki 2015c). Figure 20 shows an actual resonant response of a super high-rise building in Osaka, Japan during the 2011 off the Pacific coast of Tohoku earthquake. This phenomenon clearly indicates the necessity and requirement of consideration of response under long-duration ground motion.

The multiple impulse input can be used as a substitute of the long-duration earthquake ground motion, mostly expressed in terms of harmonic waves, and a closed-form solution can be derived of the elastic-plastic response of an SDOF structure under the critical multiple impulse input. While the critical set of input amplitude and input frequency (timing of impulse) have to be computed iteratively for the multi-cycle sinusoidal wave, that can be obtained directly without iteration for the multiple impulse input by introducing a modified version (only the timing between the first and second impulses is modified so that the second impulse is given at the zero restoring-force). The resonance can be proved by using energy investigation. The critical timing of the multiple impulses can be characterized as the time with zero restoring force. This decomposition of input amplitude and input frequency has overcome the long-time difficulty in finding the resonant frequency without repetition.

Since only the free-vibration appears in such multiple impulse input, the energy approach plays an important role in the derivation of the closed-form solution of a complicated elastic-plastic critical response. In other words the energy approach enables the derivation of the maximum critical elastic-plastic seismic response without solving the differential equation (equation of motion). In this process, the input of impulse is expressed by the instantaneous change of velocity of the structural mass. The maximum elastic-plastic response after impulse can be obtained by equating the initial kinetic energy computed by the initial velocity to the sum of hysteretic and elastic strain energies as in the formulation under the double and triple impulses.

10 CONCLUSIONS

In this paper, it has been shown that good approximate elastic-plastic responses of various structural models to near-fault ground motions and long-duration ground motions can be derived by using the responses to the corresponding double, triple and multiple impulses. The original energy approach played an important role in the derivation of such good approximate responses in closed form. It should be emphasized that even the phenomena expressed by the negative second slope can be treated in a unified manner.

11 ACKNOWLEDGEMENTS

Part of the present work is supported by the Grant-in-Aid for Scientific Research (KAKENHI) of Japan Society for the Promotion of Science (No.15H04079). This support is greatly appreciated. A recorded ground motion was provided by KiK-net.

12 REFERENCES

Alavi, B. and Krawinkler, H. 2004. Behaviour of moment resisting frame structures subjected to near-fault ground motions, *Earthquake Eng. Struct. Dyn.* **33**(6), 687–706.

Caughey, TK. 1960. Sinusoidal excitation of a system with bilinear hysteresis. *J. Appl. Mech.* **27**(4), 640–643.

Dimitrakopoulos, E. G. and DeJong, M. J. 2012. Revisiting the rocking block: closed-form solutions and similarity laws, *Proc. R. Soc. A*, **468**, 2294-2318.

Drenick, RF. 1970. Model-free design of aseismic structures. *J. Eng. Mech. Div.*, ASCE, **96**(EM4), 483-493.

Hall, J. F., Heaton, T. H., Halling, M. W., and Wald, D. J. 1995. Near-source ground motion and its effects on flexible buildings, *Earthuake Spectra*, **11**(4), 569–605.

Iwan, W. D. 1961. *The dynamic response of bilinear hysteretic systems*, Ph.D. Thesis, California Institute of Technology.

Kalkan, E. and Kunnath, S.K. 2006. Effects of fling step and forward directivity on seismic response of buildings, *Earthquake Spectra*, **22**(2), 367–390.

Khaloo, A.R., Khosravi1, H. and Hamidi Jamnani, H. 2015. Nonlinear interstory drift contours for idealized forward directivity pulses using "Modified Fish-Bone" models; *Advances in Structural Eng.***18**(5), 603-627.

Kojima, K. and Takewaki, I. 2015a. Critical earthquake response of elastic-plastic structures under near-fault ground motions (Part 1: Fling-step input), *Frontiers in Built Environment* (Specialty Section: Earthquake Engineering), Volume 1, Article 12.

Kojima, K. and Takewaki, I. 2015b. Critical earthquake response of elastic-plastic structures under near-fault ground motions (Part 2: Forward-directivity input), *Frontiers in Built Environment* (Specialty Section: Earthquake Engineering), Volume 1, Article 13.

Kojima, K. and Takewaki, I. 2015c. Critical input and response of elastic-plastic structures under long-duration earthquake ground motions, *Frontiers in Built Environment* (Specialty Section: Earthquake Engineering), Volume 1, Article 15.

Kojima, K. and Takewaki, I. 2016a. Closed-form critical earthquake response of elastic-plastic structures on compliant ground under near-fault ground motions, *Frontiers in Built Environment* (Specialty Section: Earthquake Engineering), Volume 2, Article 1.

Kojima, K. and Takewaki, I. 2016b. Closed-form dynamic stability criterion for elastic-plastic structures under near-fault ground motions, *Frontiers in Built Environment* (Specialty Section: Earthquake Engineering), Volume 2, Article 6.

Kojima, K. and Takewaki, I. 2016c. A simple evaluation method of seismic resistance of residential house under two consecutive severe ground motions with intensity 7, *Frontiers in Built Environment* (Specialty Section: Earthquake Engineering) , Volume 2, Article 15.

Makris, N and Kampas, G. 2016. Size versus slenderness: Two competing parameters in the seismic stability of free-standing rocking columns, *Bull. Seismol. Soc. Am.*, **106**(1) published online.

Mavroeidis, G. P., and Papageorgiou, A. S. 2003. A mathematical representation of near-fault ground motions, *Bull. Seism. Soc. Am.*, **93**(3), 1099-1131.

Nabeshima, K., Taniguchi, R., Kojima, K. and Takewaki, I. 2016. Closed-form overturning limit of rigid block under critical near-fault ground motions, *Frontiers in Built Environment* (Specialty Section: Earthquake Engineering), Volume 2, Article 9.

Sasani, M. and Bertero, V.V. 2000. "Importance of severe pulse-type ground motions in performance-based engineering: historical and critical review," in *Proceedings of the Twelfth World Conference on Earthquake Engineering*, Auckland, New Zealand.

Takewaki, I. 2007. *Critical excitation methods in earthquake engineering*, Elsevier, Second edition in 2013.

Taniguchi, R., Kojima, K. and Takewaki, I. 2016. Critical response of 2DOF elastic-plastic building structures under double impulse as substitute of near-fault ground motion, *Frontiers in Built Environment* (Specialty Section: Earthquake Engineering), Volume 2, Article 2.